

# Surface Change of Ras Enabling Effector Binding Monitored in Real Time at Atomic Resolution

Carsten Kötting,\* Angela Kallenbach, Yan Suveyzdis, Carolin Eichholz, and Klaus Gerwert\*[a]

*Ras*, the prototype of the *Ras* superfamily, acts as a molecular switch for cell growth. External growth signals induce a GDP-to-GTP exchange. This modifies the *Ras* surface (*Ras*<sub>on</sub>GTP) and enables effector binding, which then activates signal-transduction pathways. GTP hydrolysis, catalysed by *Ras* and GAP, returns the signal to "off" (*Ras*<sub>off</sub>GDP). Oncogenic mutations in *Ras* prevent this hydrolysis, and thereby cause uncontrolled cell growth. In the *Ras*<sub>off</sub>-to-*Ras*<sub>on</sub> transition, the *Ras* surface is changed by a movement of the switch I loop that controls effector binding. We monitored this surface change at atomic resolution in real time by time-resolved FTIR (trFTIR) spectroscopy. In the transition from

*Ras*<sub>off</sub> to *Ras*<sub>on</sub> a GTP-bound intermediate is now identified, in which effector binding is still prevented (*Ras*<sub>off</sub>GTP). The loop movement from *Ras*<sub>off</sub>GTP to *Ras*<sub>on</sub>GTP was directly monitored by the C=O vibration of Thr35. The structural change creates a binding site with a rate constant of  $5\text{ s}^{-1}$  at 260 K. A small molecule that shifted the equilibrium from the *Ras*<sub>on</sub>GTP state towards the *Ras*<sub>off</sub>GTP state would prevent effector binding, even if hydrolysis were blocked by oncogenic mutations. We present a spectroscopic fingerprint of both states that can be used as an assay in drug screening for such small molecules.

## Introduction

The guanine nucleotide-binding protein (GNBP) *Ras* regulates several signal-transduction processes involved in cell growth and differentiation.<sup>[1,2]</sup> It serves as a prototype for the superfamily of GNBP: molecular switches that cycle between the active GTP-bound state (the "on" state) and the inactive GDP-bound state (the "off" state). *Ras* interactions with downstream effectors are only possible in the "on" state (Figure 1). The in-

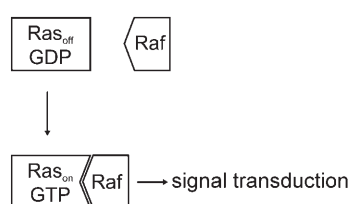


**Figure 1.** Scheme for the "on" switch of signal transduction. Only the GTP-bound state can mediate signal transduction by effector binding.

teraction with Raf mediates the best-studied pathway (via the mitogen-activated protein (MAP) kinase cascade) to activate ERK and control transcription. *Ras* can activate further signalling pathways by interaction with effectors such as phosphoinositide 3-kinases (PI3K), RALGDS or phospholipase C $\epsilon$  (PLC $\epsilon$ ). It thus influences control of survival, transcription, cytoskeletal signalling, translation, vesicle transport, cell-cycle progression, and calcium signalling.<sup>[3]</sup> The switch to "off" is accomplished by GTP hydrolysis. This process is slow for *Ras*-GTP, which allows

further control of this process by GTPase-activating proteins (GAPs).<sup>[4]</sup> The *Ras* protein has been extensively studied by various methods, including X-ray crystallography,<sup>[5–7]</sup> NMR,<sup>[8,9]</sup> theoretical methods<sup>[10–14]</sup> and FTIR.<sup>[15–21]</sup>

Time-resolved FTIR (trFTIR) difference spectroscopy monitors protein reactions at the atomic level.<sup>[22]</sup> Therefore, the GTPase is loaded with caged GTP, which cannot be hydrolyzed by *Ras*. *Ras*-GTP is formed by a laser flash, and the following hydrolysis reaction is monitored by trFTIR with a resolution of milliseconds. Whereas the frequently used NPE-caged GTP<sup>[23,24]</sup> forms GTP via an intermediate (the *aci*-nitro anion), PHP-caged GTP forms GTP directly. In the latter, the cleavage is already performed in the excited state, within 500 ps.<sup>[25]</sup> This allows a better time resolution for our measurements.

The phosphate vibrations of GTP bound to *Ras* were assigned by using  $^{18}\text{O}$ -labelled caged GTP,<sup>[16]</sup> and several aspects of the GTPase reaction were revealed. Comparison of the vibrations of GTP in water to those when bound to *Ras* showed that the  $\alpha$ -,  $\beta$ -, and  $\gamma$ -phosphate vibrations, which were highly

[a] Dr. C. Kötting, A. Kallenbach, Dr. Y. Suveyzdis, C. Eichholz, Prof. Dr. K. Gerwert  
Lehrstuhl für Biophysik, Ruhr-Universität Bochum  
44780 Bochum (Germany)  
Fax: (+49) 234-32-14238  
E-mail: carsten.koetting@rub.de  
gerwert@bph.rub.de

Supporting information for this article is available on the WWW under <http://www.chembiochem.org> or from the author.

coupled in water, became uncoupled upon binding to Ras, and the absorbance bands became narrower. This indicated that GTP was forced into a distinct conformation within the binding pocket, which induced a specific charge distribution. This charge movement is crucial for catalysis, as supported by the recent finding that the main catalytic effect of Ras is enthalpic and originates, therefore, from electrostatic interactions.<sup>[26]</sup> However, the geometry is insensitive to changes in the charge distribution. The calculated charge shift of 0.2 e upon Ras-GTP binding leads to changes in the geometry in the order of 0.01 Å.<sup>[14]</sup> TrFTIR is sensitive enough to detect these changes. For example, a change of 0.01 Å in PO bond length will change the frequency of the vibration by about 10 cm<sup>-1</sup>, which can be easily resolved.

NMR measurements with Ras bound to the nonhydrolysable GTP analogue GppNHp revealed two conformations, termed state 1 and state 2.<sup>[8,27]</sup> The T35S mutation shifts the equilibrium to state 1, but interaction with the binding domain of the effector Raf kinase (RafRBD) shifts it back to state 2. A conformation-sensitive fluorescence change of the Ras protein was also found upon binding of BeF<sub>3</sub><sup>-</sup> to Ras-GDP, for which the fluorescence lifetime of a Y32W mutant was used.<sup>[28]</sup>

Although the phosphate vibrations of Ras have been intensively studied by trFTIR spectroscopy, no vibration of the amino acids has been assigned so far. In this paper, we report spectral fingerprints for the "on" and the "off" state vibrations of the protein, and the first assignment by isotopic labelling of the Ras protein (Thr35). By means of this marker band and pHP-caged GTP,<sup>[29]</sup> we were able to measure directly the time course for the switching reaction that leads to the surface change that enables effector binding.

## Results and Discussion

### The two conformations of RasGTP observed by FTIR spectroscopy

Ras-GppNHp exists in an equilibrium between two conformations, as indicated in <sup>31</sup>P NMR experiments by the splitting of each of the α- and γ-phosphate resonance lines into two signals.<sup>[8,27]</sup> These states are termed state 1 and state 2. By adding the effector RafRBD, the equilibrium is shifted towards state 2; it might be reasonable to term this state Ras<sub>on</sub> and state 1 as Ras<sub>off</sub>. In Ras T35S, only state 1 is occupied, while adding RafRBD shifts the equilibrium towards state 2. In our time-resolved measurements, we used the natural nucleotide GTP instead of the nonhydrolysable analogue GppNHp. Unlike GppNHp, only one conformation (state 2) is observed for GTP in FTIR photolysis spectra. This observation is in accordance with ENDOR measurements with GTP.<sup>[30]</sup> In photolysis spectra of Ras-caged-GTP (Figure 2), the bands of the equilibrated Ras-GTP state point upwards, and absorptions of the Ras-caged-GTP state point downwards. By comparing the spectra of WT and T35S Ras, we see changes in α-, β-, and γ-phosphate bands; this indicates a shift to another Ras-GTP state. NMR resolves differences between WT and T35S only for the α- and γ-phosphorus resonances. In addition, in the infrared, the β

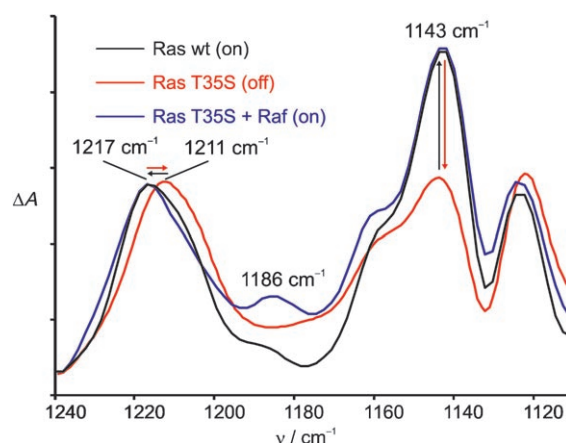


**Figure 2.** Section of the photolysis spectrum of Ras WT (black), Ras T35S (red) and Ras T35S-RafRBD (blue) showing the absorptions of the β- and γ-phosphate of the equilibrated Ras-GTP state as positive bands. NPE-caged GTP was used here.

absorption is red-shifted from 1217 to 1211 cm<sup>-1</sup> in Ras T35S. The γ band loses most of its intensity. The α band overlaps with a band of caged GTP, and will be shown later (see below). The band at 1186 cm<sup>-1</sup> does not shift upon isotopic labelling of any of the phosphate groups, and is thus assigned to a protein vibration (not yet assignable to a specific group). Upon addition of RafRBD, the phosphate absorption of the Ras WT state is recovered, again in agreement with NMR. This shows that in our measurements, by using GTP instead of GppNHp, the equilibrium is shifted completely towards the Ras<sub>on</sub> conformation (state 2), and the mutant Ras T35S is in the Ras<sub>off</sub> conformation (state 1).

In addition to the information on the phosphate groups revealed by NMR and ENDOR, trFTIR revealed information on the protein reaction. To elaborate the differences of Ras<sub>on</sub> and Ras<sub>off</sub> we calculated the double-difference spectrum of the WT photolysis spectrum (Ras<sub>on</sub>-GTP-Ras-caged-GTP) and the Ras T35S photolysis spectrum (Ras<sub>off</sub>-GTP-Ras-caged-GTP). In this spectrum

$$(\text{Ras}_{\text{on}} \cdot \text{GTP} - \text{Ras} \cdot \text{caged-GTP}) - (\text{Ras}_{\text{off}} \cdot \text{GTP} - \text{Ras} \cdot \text{caged-GTP}) = (\text{Ras}_{\text{on}} \cdot \text{GTP} - \text{Ras}_{\text{off}} \cdot \text{GTP})$$

the Ras-caged-GTP bands cancelled (they are both Ras<sub>off</sub>, see below) and a difference spectrum of Ras<sub>on</sub>-GTP-Ras<sub>off</sub>-GTP resulted. We found changes for all three phosphate bands and, additionally, in the amide region (Figure 3; the Ras<sub>on</sub> bands face upwards, the Ras<sub>off</sub> bands face downwards). Both states give sharp bands with similar half-widths. This indicates that not only the Ras<sub>on</sub> but also the Ras<sub>off</sub> state has an ordered conformation. In most crystal structures, the "on" state is observed. In structures that should have the "off" state various conformations of the switch-regions are often found; this leads to the concept of an "unordered" state. But this seems to be caused by crystallization artifacts, because open loops interact with neighbouring Ras molecules in the crystal.

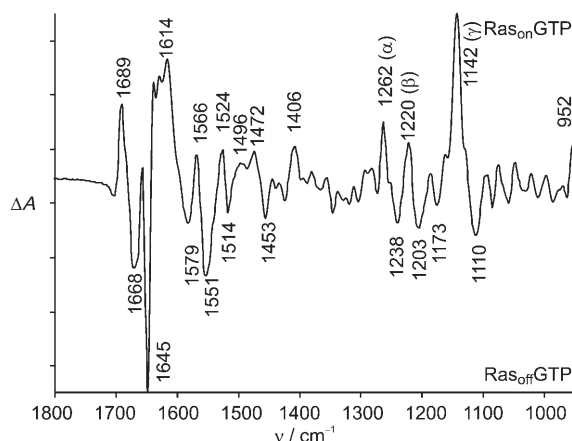


**Figure 3.** Double-difference spectrum between Ras<sub>on</sub>GTP and Ras<sub>off</sub>GTP, calculated as detailed in the text. Positive peaks are due to the Ras<sub>on</sub>GTP state, negative to the Ras<sub>off</sub>GTP state. The wavenumbers for the most intense bands of both states are given.

### TrFTIR resolves the switching process

Measuring the formation of Ras-GTP from Ras-caged-GTP, by using the pHP cage, reveals a novel rate of about  $5 \text{ s}^{-1}$  (Figure 4A). This was not resolved with the NPE cage, because GTP is formed at a slower rate of  $2 \text{ s}^{-1}$  (Figure 4B). This rate is absent in the photolysis of Ras T35S-pHP-caged GTP (Figure 4A), but in T35S with RafRBD it is recovered. We conclude that Ras<sub>off</sub>GTP is formed after photolysis, and that the additional rate in the presence of RafRBD reflects the switch towards Ras<sub>on</sub>GTP. The state formed in Ras WT directly after photolysis, but before the conformational change, is the same (Ras<sub>off</sub>GTP) as that which persists until hydrolysis in Ras T35S (see Figure S1 in the Supporting Information). Again the bands of the protein groups are nicely resolved in the amplitude spectrum of the  $5 \text{ s}^{-1}$  rate of Ras WT, and they are indeed almost identical to the Ras<sub>off</sub>–Ras<sub>on</sub> spectra shown in Figure 5. This proves that we monitored directly the conformational change from Ras<sub>off</sub>GTP to Ras<sub>on</sub>GTP. The activation parameters for this rate (with GppNhp) had been previously estimated by means of NMR line shape analysis.<sup>[31]</sup> Extrapolation of these results by using transition state theory yielded (in agreement) a rate of  $9 \text{ s}^{-1}$  at 260 K.

### Switching process initiated by binding of berylliumfluoride

$\text{BeF}_3^-$  can mimic the missing  $\gamma$ -phosphate in proteins bound to ADP or GDP (for example, in F-actin,<sup>[32]</sup> transducin<sup>[33]</sup> and Cdc42Hs<sup>[34]</sup>). The structure of myosin complexed with ADP +  $\text{BeF}_3^-$  has been solved by X-ray crystallography.<sup>[35]</sup> In this structure, the distance between the  $\beta$ -P and Be atoms is 2.89 Å, similar to the distance between  $\beta$  and  $\gamma$  phosphorus atoms in, for example, Ras-GTP.<sup>[6]</sup> Furthermore, the Be–F bond lengths and the tetrahedral coordination of the Be atom are very similar to the equivalents in the  $\gamma$ -phosphate of ATP. Thus GDP· $\text{BeF}_3^-$  can be considered as a ground state analogue. The association of  $\text{BeF}_3^-$  with RasY32W-GDP was measured by Diaz et al. by using fluorescence spectroscopy<sup>[28]</sup> to derive the ener-

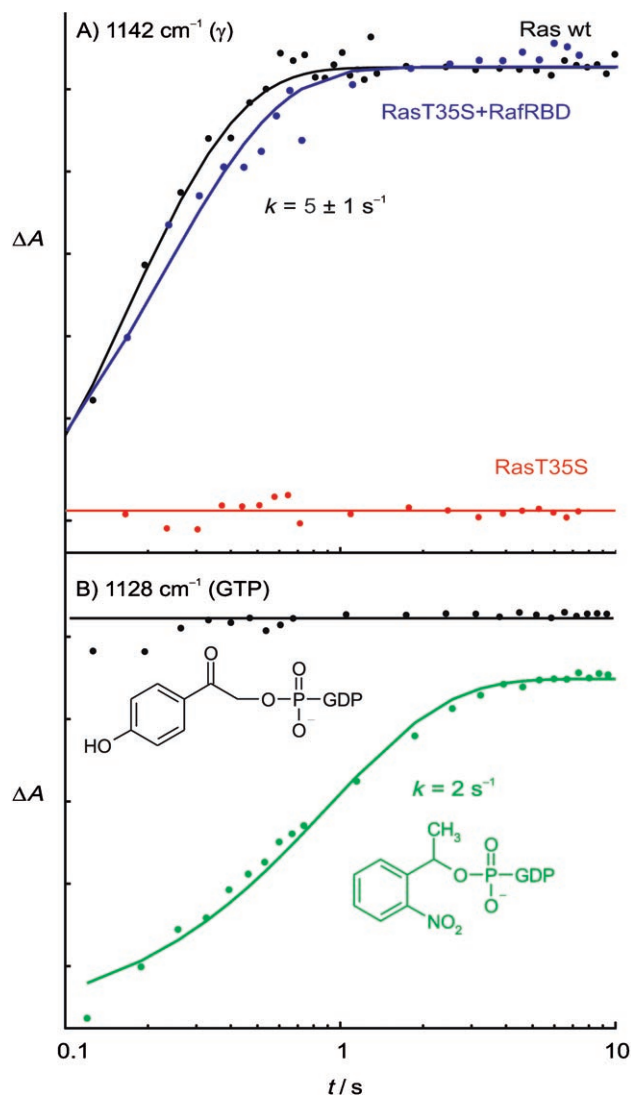


**Figure 4.** GTP absorption changes after irradiation of caged-GTP. A) Absorbance changes after irradiation of pHP-caged-GTP bound to Ras WT (black), Ras T35S (red) and Ras T35S-RafRBD (blue) for a marker band of the Ras<sub>on</sub>GTP state. Ras WT and Ras T35S-RafRBD form the “on” state with a rate of  $5 \text{ s}^{-1}$ , whereas Ras T35S shows no reaction. B) GTP in water. Whereas formation of GTP from pHP-caged-GTP (black) is already complete by the first data point, formation of GTP from NPE-caged-GTP (green) takes place with a rate constant of  $2 \text{ s}^{-1}$ .

gies and rate constants for the association. Two rates were found: the first was assigned to the complex formation and the second, with a rate of  $2 \text{ s}^{-1}$  at 288 K, to a conformational change of the protein. We measured the formation of the analogous complex by FTIR. Ras-caged-GDP was photolysed in the presence of  $\text{Be}^{2+}$  and  $\text{F}^-$  ions, and we observed the incorporation of, most likely,  $\text{BeF}_3^-$  with a rate of about  $0.5 \text{ s}^{-1}$  at 260 K. Besides significant changes in the phosphate region, we also observed a conformational change of the protein. This difference spectrum is also shown in Figure 5. Again it agrees with the other two spectra presenting the differences of the Ras<sub>off</sub> and the Ras<sub>on</sub> states. This proves that the conformational change reflects the switching of the Ras protein from “off” to “on”. Thus, the protein conformation of Ras-GDP is the same as

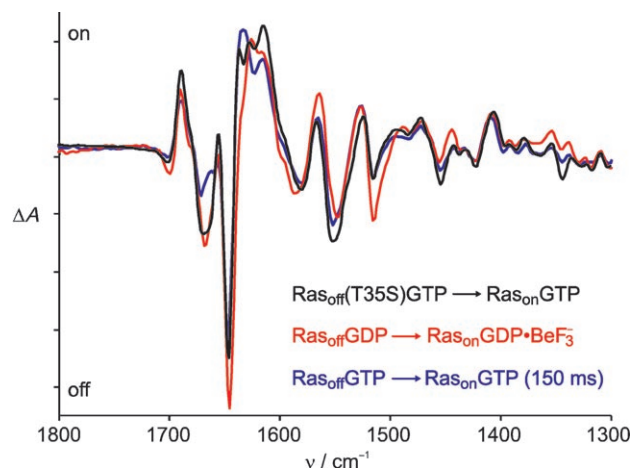


**Figure 5.** The spectroscopic fingerprint of the  $Ras_{on}$  and  $Ras_{off}$  states obtained by three independent experiments: Black: double difference as given in Figure 2. Blue: amplitude spectrum of the reaction observed after photolysis of  $Ras\text{-}pHP\text{-}caged\text{-}GTP$ . Red: amplitude spectrum of the reaction assigned to the binding of  $BeF_3^-$  to  $Ras\text{-}GDP$ . Bands facing upwards are due to the “on” state, bands facing downwards are due to the “off” state. For the corresponding spectra, including the phosphate region, see Figure S2.

$Ras\text{-}caged\text{-}GTP$  or  $Ras\ T35S\text{-}GTP$ ; in particular, in  $Ras_{off}\text{-}GTP$  the protein has the same conformation as  $Ras_{off}\text{-}GDP$ . On the other hand,  $Ras_{on}\text{-}GTP$  has the same conformation as  $Ras\text{-}GDP\text{-}BeF_3^-$ ; this demonstrates that the latter is a good mimic when used in fluorescence measurements or X-ray structures.

#### Assignment of the amide I vibration of Thr35

In order to obtain more information about the two structures, we had to assign the bands in our spectra to amino acids. Since many mutants are too invasive, we assigned the bands by isotopic labelling, which is noninvasive and shifts only the vibrations of the marked group. The shifts are easily identified by comparing the spectra of the unlabelled and the labelled protein. We produced  $Ras$  in M9 medium with isotopically labelled Thr. Although all eleven threonines (2, 19, 35, 50, 58, 74, 87, 124, 144, 148, 158) of  $Ras$  are labelled, we expect only the absorptions of Thr35 to show up in the difference spectrum. By comparing the  $Ras\text{-}GDP$  and  $Ras\text{-}GTP$  structural models, Thr35 is the only threonine within the protein that is expected to change (p-loop, switch I, switch II) and could give rise to absorbance changes. Thr35 is expected to be a key residue in the switch reaction.<sup>[35]</sup> In Figure 6 the difference spectra of the labelled and the unlabelled protein are compared. The band at  $1689\text{ cm}^{-1}$  is shifted upon labelling, and can clearly be assigned to threonine, most likely to Thr35. In this region only the  $C=O$  amide I backbone of Thr absorbs. The shifted band at around  $1645\text{ cm}^{-1}$  in the labelled spectrum is not observed as clearly. It is masked by an additional negative band in the spectral region, which is distorted by the strong background absorbance of water and amide I vibrations. In  $D_2O$ , the background absorbance is reduced and the data quality is improved, thus revealing the band shift in the double difference spectrum (shown in the inset). The band is slightly shifted to

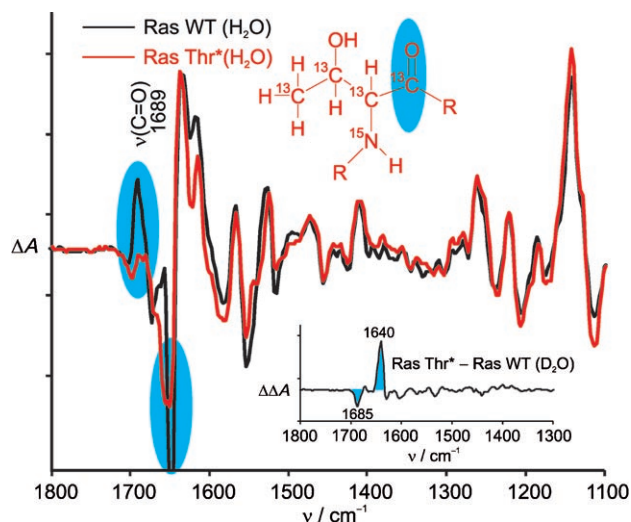


**Figure 6.** Amplitude spectra of the switching reactions (blue in Figure 5) for  $Ras$  (black), and  $Ras$  with  $^{13}C\ ^{15}N$ -labelled threonine (red). The band at  $1689\text{ cm}^{-1}$  is assigned to the carbonyl stretching vibration of unlabelled Thr35. In the inset the corresponding double difference spectrum ( $Ras\ (^{13}C\ ^{15}N\text{-threonine}) - Ras$ ) is shown. Here the position of the absorption of the labelled Thr35 can be seen. The region around  $1650\text{ cm}^{-1}$  is usually disturbed by the strong water absorption, thus the double difference spectrum was obtained by using  $D_2O$ , leading to the small red-shift of the carbonyl vibration,  $4\text{ cm}^{-1}$ .

$1685\text{ cm}^{-1}$  due to  $D_2O$  for unlabelled threonine, and it is further downshifted to  $1640\text{ cm}^{-1}$  due to labelling. The intensity of the shifted band does not match exactly the intensity of the unshifted band, possibly due to coupling with other amide I bands.

The absorption of Thr35 at  $1689\text{ cm}^{-1}$  is at an unusually high wavenumber for an amide I vibration, indicating only weak hydrogen bonding<sup>[37]</sup> in the  $Ras_{on}$  state: The energy of the amide I bond is strongly influenced by hydrogen bonding. For example, in the model compound  $N$ -methylacetamide, the corresponding vibration is at  $1723\text{ cm}^{-1}$  in the gas phase, but at  $1625\text{ cm}^{-1}$  in water.<sup>[38]</sup> Since there are two lone-pair molecular orbitals at the carbonyl oxygen, this group can act as an acceptor for two strong hydrogen bonds. According to *ab initio* calculations, the hydration enthalpy is about  $10\text{ kcal mol}^{-1}$ .<sup>[39]</sup> Since frequencies can correlate linearly with bond length, one can estimate an energy gain of about  $0.15\text{ kcal mol}^{-1}\text{ cm}^{-1}$ . Thus, a blue shift of the band by approximately  $30\text{ cm}^{-1}$ , as estimated here, gives a stored energy of about  $5\text{ kcal mol}^{-1}$ . Vetter and Wittinghofer referred to the  $GTP$ -hydrolysis as a “loaded spring” mechanism.<sup>[36]</sup> Energy for this spring might be stored in this carbonyl bond. The closest potential hydrogen bond donor in the X-ray structure of  $Ras\text{-}GppNHp$  is the nucleophilic water (water 175 in structure 5P21<sup>[40]</sup>). According to our results, its hydrogens are not coordinated to Thr35 but to other residues, such as the  $\gamma$ -phosphate oxygens or Gly60.

Note that an assignment of the Thr35 band by site-directed mutagenesis is not possible, because mutants cause a shift towards the  $Ras_{off}$  state. This does not lead only to a specific change of the bands of residue 35, but to a major change of the spectrum as shown in Figure 3. Further, only the vibrations



of side groups, not the backbone, can be assigned by site-directed mutagenesis.

### Surface change of Ras

We measured the switching reaction in a time-resolved manner and found a rate constant of  $5\text{ s}^{-1}$  at 260 K (Figure 7A). The changes within the GTP bands (with  $\gamma$ -GTP at  $1143\text{ cm}^{-1}$  as a marker) occur with the same kinetics as the changes of the switch I region (absorption of Thr35 at  $1689\text{ cm}^{-1}$  as a marker). This demonstrates that the conformational change, which is necessary for effector-binding, occurs after GTP binding with  $\text{Ras}_{\text{off}}\text{GTP}$  as an intermediate (Figure 7B).

Due to the lack of structural information for the switch regions (for example, in the  $\text{Ras}_{\text{off}}\text{T35S}$  structure<sup>[8]</sup>), it was assumed that this structure is not well defined. However, the spectrum of the "off" state, and its similarity across all Ras mutants, shows that this state is probably much more ordered than previously thought. This finding is supported by a recent X-ray structure of M-Ras<sup>[41]</sup> (Figure 7C). M-Ras is believed to have the "off" conformation, because it shows only one conformation (state 1) in  $^{31}\text{P}$  NMR analysis, and the resonances are similar to those assigned to the "off" state for H-Ras. The switch I region of the protein is also resolved in this X-ray structure. The  $\text{Ras}_{\text{off}}$  structure clashes with the effector because the switch I loop is pointing outwards (Figure 7D). The assignment of the Thr35 band enables us to monitor directly the movement of switch I. The surface change enabling effector-binding, as shown in Figure 7C, has a rate of  $5\text{ s}^{-1}$ .

### FTIR assay for the switch

Since we have assigned spectral fingerprints to the two Ras conformations, it is now possible to investigate further Ras mutants, whether they are switching to the "off" or the "on" state. This can be achieved by a simple assay, measuring the photolysis spectrum and comparing the marker bands as given in Figure 2. We used this simple assay to examine some Ras mutants. Interestingly, many mutants of switch I (Y32F, Y32W, Y32R, P34R, T35S, T35A, D38A, D38E) and switch II (A59T) are found to switch to the  $\text{Ras}_{\text{off}}$  state. (The corresponding double-difference spectra are given in Figure S3.) This indicates that a complex hydrogen bonded network exists, and that changes in one of the regions will probably destroy this network. This tendency of mutants to switch towards the "off" state might function as a safety system (to prevent them from being oncogenic). The residues involved are shown in Figure 8. Further evidence is offered by the extreme loss of intensity of the  $\gamma$ -phosphate vibration, compared  $\text{Ras}_{\text{on}}\text{GTP}$  and  $\text{Ras}_{\text{off}}\text{GTP}$ . Where-

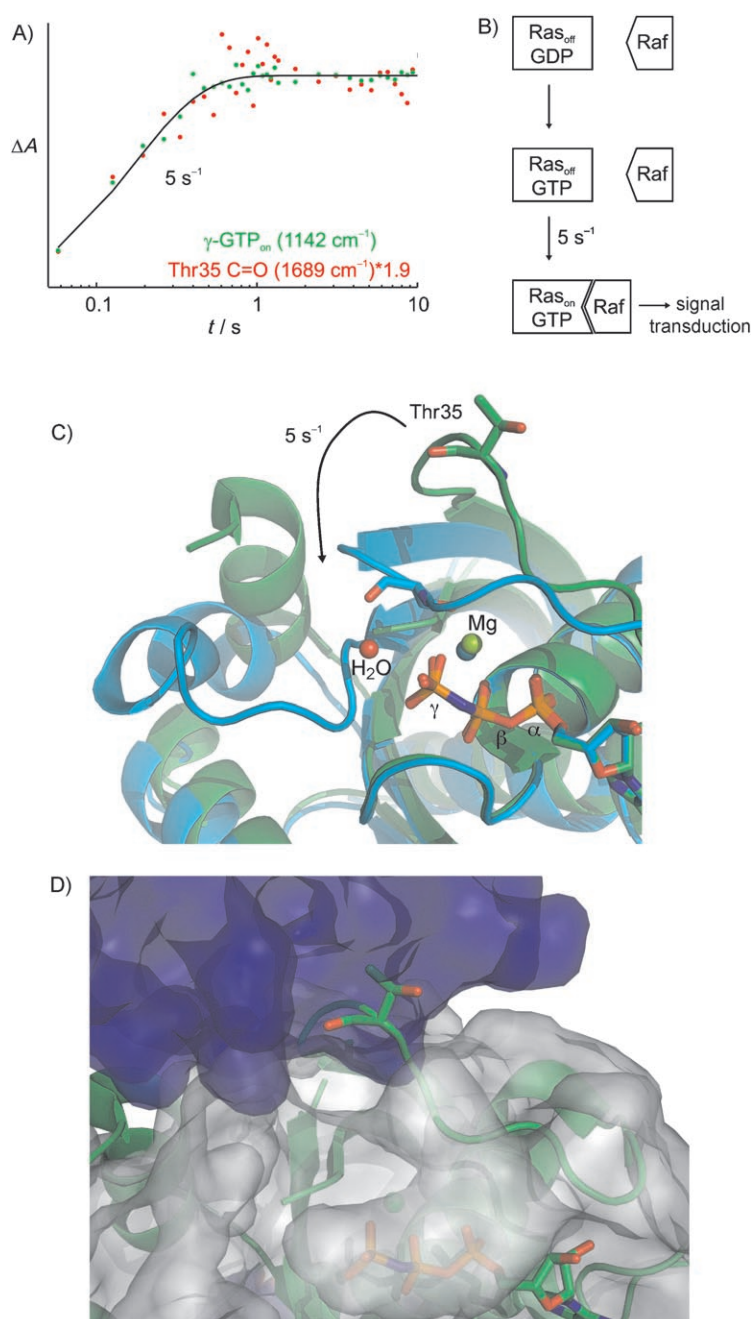


**Figure 7.** A) Kinetics of the "on" switch demonstrated on the basis of the changes of the nucleotide ( $\gamma$ -GTP<sub>on</sub> as a marker) and the switch I (Thr35 backbone vibration as a marker), respectively. Both changes are performed with the same rate of  $5\text{ s}^{-1}$ . B) Scheme for the "on" switch of signal transduction based on our results: After GTP binding,  $\text{Ras}_{\text{off}}\text{GTP}$  is formed, which subsequently accomplishes the conformational change in order to mediate signal transduction by effector binding. C) Comparison of the  $\text{Ras}_{\text{on}}$  (cyan, PDB ID: 5P21<sup>[40]</sup>) and the  $\text{Ras}_{\text{off}}$  (green, PDB ID: 1X1S<sup>[41]</sup>) structures obtained by X-ray crystallography. The nucleotides are superimposed. The large movement of Thr35 is highlighted. D) Overlay of the Ras-effector complex (Ras: white surface, effector Byr2RBD: blue surface, PDB ID: 1K8R<sup>[48]</sup>) with the  $\text{Ras}_{\text{off}}$  structure (green cartoon). The switch I region around Thr35 of the  $\text{Ras}_{\text{off}}$  structure clashes with the effector.

as in the "on" state only one distinct conformation of this group is possible, in the "off" state multiple conformations are possible, due to rotation around the  $\beta$ - $\gamma$  bridge and/or the

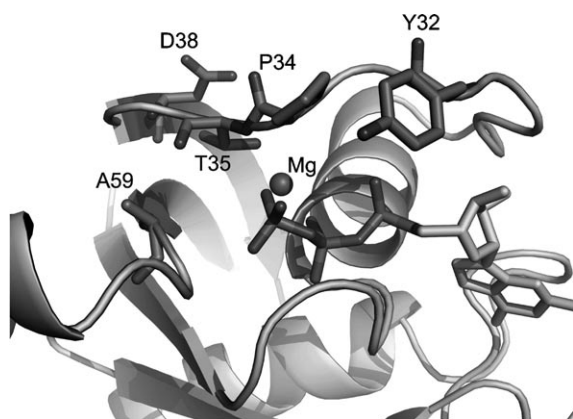


**Figure 8.** Ras with indication of the residues which upon mutation force the Ras<sub>off</sub> state. These are residues of switch I, switch II, and the Mg ion. Together they form a pocket around the phosphates.

accessibility of bulk water. Note that GTP in water also has much broader absorptions.

In conclusion, we have monitored the Ras<sub>off</sub>GTP-to-Ras<sub>on</sub>GTP transition by time-resolved FTIR spectroscopy. By means of isotopic labelling, we assigned a vibration to Thr35 in the switch I loop. Following the Thr35 absorbance change, we monitored the surface change of Ras that enables effector binding. A small molecule that is able to shift the equilibrium towards Ras<sub>off</sub> might work in a molecular cancer therapy.<sup>[42]</sup> Our assay can screen for such small molecules. The approach can be applied to other GTPases and ATPases.

## Experimental Section

The P<sup>3</sup>-1-(2-nitrophenyl)ethyl ester of GTP was synthesized in two steps from 2-nitrophenylacetylhydrazide and GTP with subsequent purification via anion-exchange chromatography according to a procedure by Walker and Trentham.<sup>[23]</sup>

The P<sup>3</sup>-*para*-hydroxyphenacyl ester of GTP was synthesized by coupling GDP and pHP-caged P<sub>i</sub>. The latter was obtained in five steps from *para*-hydroxy-acetophenone and dibenzylphosphate, according to a procedure by Park and Givens.<sup>[29]</sup>

Wild-type and mutants of H-Ras<sup>[43]</sup> and RafRBD<sup>[44]</sup> were prepared with an *Escherichia coli* expression system.

For the FTIR measurements, Ras was loaded with the desired caged nucleotide according to John et al.<sup>[45]</sup> The sample composition was a 1:1 complex of Ras with the caged nucleotide (10 mM), MgCl<sub>2</sub> (25 mM), DTT (10 mM), and HEPES (pH 7.5, 200 mM). Photolysis experiments were performed at 260 K with 12% ethylene glycol to prevent freezing. For the measurements of the BeF<sub>3</sub><sup>-</sup> association, Ras-caged GDP (5 mM), BeSO<sub>4</sub> (50 mM), NaF (200 mM), MES (pH 6.0, 200 mM), MgCl<sub>2</sub> (20 mM), DTT (20 mM) and ethylene glycol (12%) were used. For the D<sub>2</sub>O experiments, the samples were concentrated and rehydrated in D<sub>2</sub>O (3×), and [D<sub>2</sub>]ethylene glycol was used.

The samples were prepared between two CaF<sub>2</sub> windows as detailed by Cepus.<sup>[17]</sup> Photolysis of the caged compounds was performed by an LPX 240 XeCl excimer laser (308 nm, Lambda Physics, Göttingen, Germany). 12 flashes within 24 ms were used for the pHP-cage group, and 40 flashes within 80 ms for the NPE-cage.

More than 90% of each sample is photolysed under these conditions. A modified Bruker IFS 66v/s spectrometer (Ettlingen, Germany) in the fast scan mode<sup>[46]</sup> was used for the measurement. Data acquisition was performed in the "double sided forward backward" mode; the four spectra calculated from each complete cycle of the scanner were averaged (~60 ms, 4 cm<sup>-1</sup> resolution). The first data point is at ~50 ms.

The data were analysed between 1800 and 950 cm<sup>-1</sup> with a global fit method.<sup>[47]</sup> In this analysis, the absorbance changes  $\Delta A$  are analysed with sums of  $n_r$  exponentials with apparent rate constants  $k_i$  and amplitudes  $a_i$ :

$$\Delta A(\nu, t) = \sum_{i=1}^{n_r} a_i(\nu) e^{-k_i t} + a_{\infty}(\nu)$$

In the Figures negative amplitude spectra ( $-a_i(\nu)$ ) are shown; the disappearing bands face downwards and the appearing bands face upwards.

An amplitude spectrum  $a_0(\nu)$ , calculated by

$$a_0(\nu) = a_{\infty}(\nu) - \sum_{i=1}^{n_r} a_i(\nu)$$

compares the state before the triggering of the reaction by the irradiation with the state after the flashes, extrapolated to time  $t=0$ . This is the photolysis spectrum. If there is a subsequent conformational change with rate  $k_1$  the equilibrated photolysis spectrum is given by  $a_0(\nu) + a_1(\nu)$ .

Isolation of isotopically labelled Ras was done by using a modified M9 medium. Incorporation was checked by mass spectrometry and was greater than 95%. Details will be given in a separate publication.

## Acknowledgements

We thank Alfred Wittinghofer and Christian Herrmann for providing the RasT35S plasmid, several Ras mutants, RafRBD and helpful discussions. We acknowledge Christoph Allin for performing experiments with RasGDP and Berylliumfluoride, and Henrik te Heesen for useful discussions. Support by the DFG SFB 642 is gratefully acknowledged.

**Keywords:** cage compounds • GTPases • IR spectroscopy • proteins • time-resolved spectroscopy

- [1] A. Wittinghofer, *Biol. Chem.* **1998**, 379, 933–937.
- [2] A. Singh, A. P. Sowjanya, G. Ramakrishna, *FASEB J.* **2005**, 19, 161–169.
- [3] J. Downward, *Nat. Rev. Cancer* **2003**, 3, 11–22.
- [4] M. R. Ahmadian, U. Hoffmann, R. S. Goody, A. Wittinghofer, *Biochemistry* **1997**, 36, 4535–4541.
- [5] K. Scheffzek, M. R. Ahmadian, W. Kabsch, L. Wiesmüller, A. Lautwein, F. Schmitz, A. Wittinghofer, *Science* **1997**, 277, 333–338.
- [6] A. J. Scheidig, C. Burmester, R. S. Goody, *Structure* **1999**, 7, 1311–1324.
- [7] A. J. Scheidig, S. M. Franken, J. E. T. Corrie, G. P. Reid, A. Wittinghofer, E. F. Pai, R. S. Goody, *J. Mol. Biol.* **1995**, 253, 132–150.
- [8] M. Spoerner, C. Herrmann, I. R. Vetter, H. R. Kalbitzer, A. Wittinghofer, *Proc. Natl. Acad. Sci. USA* **2001**, 98, 4944–4949.
- [9] M. Rohrer, T. F. Prisner, O. Brüggemann, H. Käss, M. Spoerner, A. Wittinghofer, H. R. Kalbitzer, *Biochemistry* **2001**, 40, 1884–1889.
- [10] A. Cavalli, P. Carloni, *J. Am. Chem. Soc.* **2002**, 124, 3763–3768.
- [11] N. Futatsugi, M. Tsuda, *Biophys. J.* **2001**, 81, 3483–3488.

- [12] T. M. Glennon, J. Villà, A. Warshel, *Biochemistry* **2000**, *39*, 9641–9651.
- [13] M. Kosloff, Z. Selinger, *J. Mol. Biol.* **2003**, *331*, 1157–1170.
- [14] M. Klähn, J. Schlitter, K. Gerwert, *Biophys. J.* **2005**, *88*, 3829–3844.
- [15] C. Allin, M. R. Ahmadian, A. Wittinghofer, K. Gerwert, *Proc. Natl. Acad. Sci. USA* **2001**, *98*, 7754–7759.
- [16] C. Allin, K. Gerwert, *Biochemistry* **2001**, *40*, 3037–3046.
- [17] V. Cepus, A. J. Scheidig, R. S. Goody, K. Gerwert, *Biochemistry* **1998**, *37*, 10263–10271.
- [18] H. Cheng, S. Sukal, H. Deng, T. S. Leyh, R. Callender, *Biochemistry* **2001**, *40*, 4035–4043.
- [19] X. Du, H. Frei, S.-H. Kim, *J. Biol. Chem.* **2000**, *275*, 8492–8500.
- [20] J. H. Wang, D. G. Xiao, H. Deng, M. R. Webb, R. Callender, *Biochemistry* **1998**, *37*, 11106–11116.
- [21] C. Kötting, M. Blessenohl, Y. Suveyzdis, R. S. Goody, A. Wittinghofer, K. Gerwert, *Proc. Natl. Acad. Sci. USA* **2006**, *103*, 13911–13916.
- [22] C. Kötting, K. Gerwert, *ChemPhysChem* **2005**, *6*, 881–888.
- [23] J. W. Walker, G. P. Reid, J. A. McCray, D. R. Trentham, *J. Am. Chem. Soc.* **1988**, *110*, 7170–7177.
- [24] A. Barth, J. E. T. Corrie, M. J. Gradwell, Y. Maeda, W. Mäntele, T. Meier, D. R. Trentham, *J. Am. Chem. Soc.* **1997**, *119*, 4149–4159.
- [25] A. P. Pelliccioli, J. Wirz, *Photochem. Photobiol. Sci.* **2002**, *1*, 441–458.
- [26] C. Kötting, K. Gerwert, *Chem. Phys.* **2004**, *307*, 227–232.
- [27] M. Spoerner, A. Nuehs, P. Ganser, C. Herrmann, A. Wittinghofer, H. R. Kalbitzer, *Biochemistry* **2005**, *44*, 2225–2236.
- [28] J. F. Díaz, A. Sillen, Y. Engelborghs, *J. Biol. Chem.* **1997**, *272*, 23138–23143.
- [29] C.-H. Park, R. S. Givens, *J. Am. Chem. Soc.* **1997**, *119*, 2453–2463.
- [30] M. Spoerner, T. F. Prisner, M. Bennati, M. M. Hertel, N. Weiden, T. Schweins, H. R. Kalbitzer, *Magn. Reson. Chem.* **2005**, *43*, S74–S83.
- [31] M. Geyer, T. Schweins, C. Herrmann, T. Prisner, A. Wittinghofer, H. R. Kalbitzer, *Biochemistry* **1996**, *35*, 10308–10320.
- [32] C. Combeau, M.-F. Carlier, *J. Biol. Chem.* **1989**, *264*, 19017–19021.
- [33] B. Antonny, M. Chabre, *J. Biol. Chem.* **1992**, *267*, 6710–6718.
- [34] G. R. Hoffman, N. Nassar, R. E. Oswald, R. A. Cerione, *J. Biol. Chem.* **1998**, *273*, 4392–4399.
- [35] A. J. Fisher, C. A. Smith, J. B. Thoden, R. Smith, K. Sutoh, H. M. Holden, I. Rayment, *Biochemistry* **1995**, *34*, 8960–8972.
- [36] I. R. Vetter, A. Wittinghofer, *Science* **2001**, *294*, 1299–1304.
- [37] W. Herrebout, K. Clou, H. O. Desseyn, N. Bleton, *Spectrochim. Acta Part A* **2003**, *59*, 47–59.
- [38] J. Kubelka, T. A. Keiderling, *J. Phys. Chem. A* **2001**, *105*, 10922–10928.
- [39] J. J. Dannenberg, *J. Phys. Chem. A* **2006**, *110*, 5798–5802.
- [40] E. F. Pai, U. Krengel, G. A. Petsko, R. S. Goody, W. Kabsch, A. Wittinghofer, *EMBO J* **1990**, *9*, 2351–2359.
- [41] M. Ye, F. Shima, S. Muraoka, J. Liao, H. Okamoto, M. Yamamoto, A. Tamura, N. Yagi, T. Ueki, T. Kataoka, *J. Biol. Chem.* **2005**, *280*, 31267–31275.
- [42] M. Spoerner, T. Graf, B. König, H. R. Kalbitzer, *Biochem. Biophys. Res. Commun.* **2005**, *334*, 709–713.
- [43] J. Tucker, G. Sczakiel, J. Feuerstein, J. John, R. S. Goody, A. Wittinghofer, *EMBO J* **1986**, *5*, 1351–1358.
- [44] C. Herrmann, G. A. Martin, A. Wittinghofer, *J. Biol. Chem.* **1995**, *270*, 2901–2905.
- [45] J. John, R. Sohmen, J. Feuerstein, R. Linke, A. Wittinghofer, R. S. Goody, *Biochemistry* **1990**, *29*, 6058–6065.
- [46] K. Gerwert, G. Souvignier, B. Hess, *Proc Natl Acad Sci USA* **1990**, *87*, 9774–9778.
- [47] B. Hessling, G. Souvignier, K. Gerwert, *Biophys. J.* **1993**, *65*, 1929–1941.
- [48] K. Scheffzek, P. Grünwald, S. Wohlgemuth, W. Kabsch, H. Tu, M. Wigler, A. Wittinghofer, C. Herrmann, *Structure* **2001**, *9*, 1043–1050.

Received: December 19, 2006

Published online on March 27, 2007